

# Improvement of Solubility and Oral Bioavailability of 2-(*N*-Cyanoimino)-5- $\{$ (*E*)-4-styrylbenzylidene $\}$ -4-oxothiazolidine (FPFS-410) with Antidiabetic and Lipid-Lowering Activities in Dogs by 2-Hydroxypropyl- $\beta$ -cyclodextrin

Takumi HARA, Fumitoshi HIRAYAMA, Hidetoshi ARIMA, Yoshihiro YAMAGUCHI, and Kaneto UEKAMA\*

Graduate School of Pharmaceutical Sciences, Kumamoto University; 5-1 Oe-honmachi, Kumamoto 862-0973, Japan.

Received October 3, 2005; accepted December 2, 2005; published online December 7, 2005

2-(*N*-Cyanoimino)-5- $\{$ (*E*)-4-styrylbenzylidene $\}$ -4-oxothiazolidine (FPFS-410) is a newly synthesized thiazolidine derivative having not only antidiabetic but also lipid-lowering activities. However, this compound has an extremely low aqueous solubility ( $2.8 (\pm 0.33) \times 10^{-8}$  M ( $0.0094 \pm 0.0011$   $\mu$ g/ml) in 1.0 M phosphate buffer (pH 7.0) at 25 °C). In this study, we investigated the effect of various hydrophilic cyclodextrins (CyDs) on the solubility of FPFS-410 to select a CyD suitable for formulations of the compound. Among various CyDs, 2-hydroxypropyl- $\beta$ -CyD (HP- $\beta$ -CyD) had the highest solubilizing ability to FPFS-410, *e.g.*, the solubility of the compound was increased 200000-fold by the addition of 40 mM HP- $\beta$ -CyD, which was attributable to the formation of the 1 : 2 (guest : host) inclusion complexes. The interaction of HP- $\beta$ -CyD with FPFS-410 was studied using  $^1$ H-nuclear magnetic resonance (NMR) spectroscopies including ROESY spectroscopy and a molecular modeling calculation. These results suggested that HP- $\beta$ -CyD forms a 1 : 2 (guest : host) inclusion complex with FPFS-410 by including both the stilbene and thiazolidine moieties. FPFS-410/HP- $\beta$ -CyD solid complexes with various stoichiometries were prepared by the spray drying and cogrinding methods, and confirmed by powder X-ray diffractometry that these complexes are in an amorphous state. The dissolution of FPFS-410 in water was significantly accelerated by the complexation with HP- $\beta$ -CyD. *In vivo* studies revealed that HP- $\beta$ -CyD markedly increases the bioavailability of FPFS-410 after oral administration in dogs. The present results suggest that HP- $\beta$ -CyD is useful for improvement of the extremely low bioavailability of FPFS-410.

**Key words** 2-hydroxypropyl- $\beta$ -cyclodextrin; FPFS-410; inclusion complex; solubility; dissolution; bioavailability

Diabetes mellitus is classified into two groups, non-insulin-dependent diabetes mellitus (NIDDM) and insulin-dependent diabetes mellitus (IDDM). Since insulin resistance has been acquired in NIDDM patients, insulin, its analogues and sulfonylureas cannot lower serum glucose levels sufficiently. In addition, insulin resistance contributes to the hyperglycemic state in about 80–85% of patients with this disorder.<sup>1,2)</sup> Complication of diabetes mellitus and hyperlipidemia is associated with increasing the risk of atherosclerosis. Thiazolidinedione class of drugs (TZDs), such as rosiglitazone and pioglitazone, are new type of antidiabetic agents. TZDs significantly reduce fasting plasma glucose levels by improving insulin sensitivity in NIDDM patients.<sup>3,4)</sup> Furthermore, TZDs were reported to improve lipid metabolism in NIDDM patients.<sup>5,6)</sup> TZDs are reported to influence several processes that increase cell sensitivity to insulin,<sup>7,8)</sup> including activation of peroxisome proliferator-activated receptor  $\gamma$  (PPAR $\gamma$ ),<sup>9,10)</sup> although their mechanism has not been fully elucidated. TZDs are widely used in clinical practice, but in some cases they cause weight gain, plasma volume expansion, edema or hepatotoxicity.<sup>11,12)</sup> Because these unwelcome effects of TZDs are supposed to be due to activation of PPAR $\gamma$ , various intensive attempts have been conducted to search drug candidates with potent antidiabetic and lipid-lowering activities, but with low affinity to PPAR $\gamma$ .

2-(*N*-Cyanoimino)-5- $\{$ (*E*)-4-styrylbenzylidene $\}$ -4-oxothiazolidine (FPFS-410) (Fig. 1, molecular weight 331.4), a newly synthesized cyanoimino-oxothiazolidine with improving insulin sensitivity, has shown potent lowering effects on serum glucose and triglyceride at the preclinical stage. Furthermore, FPFS-410 has much less potency for PPAR $\gamma$  acti-

vation compared with pioglitazone and does not cause body weight gain in rodents.<sup>13)</sup> Despite these valuable features, FPFS-410 exhibits an extremely low aqueous solubility ( $2.8 (\pm 0.33) \times 10^{-8}$  M ( $0.0094 \pm 0.0011$   $\mu$ g/ml) in 1.0 M phosphate buffer (pH 7.0) at 25 °C), which is a drawback for its practical use.

Cyclodextrins (CyDs) are cyclic oligosaccharides consisting of usually six, seven, or eight glucose units ( $\alpha$ -,  $\beta$ -,  $\gamma$ -CyDs, respectively) bound by 1,4-glycosidic linkages. CyDs form inclusion complexes with lipophilic drugs and improve their water solubility, dissolution rate and bioavailability.<sup>14–16)</sup> However, the solubilization effect of CyDs on drugs is dependent on the interaction strength between guest and host molecules, *i.e.*, cavity size of CyDs, spatial fitness of guest/host molecules, stoichiometry of complex, hydrophobicity of guest molecule, *etc.* Therefore, when a drug is to be formulated as CyD complex, it is important to select the most suitable CyD for the drug. Recently, various kinds of  $\beta$ -CyD derivatives have been developed to enhance the inclusion property and solubility of parent  $\beta$ -CyD and to improve pharmaceutical properties of drugs through the CyD

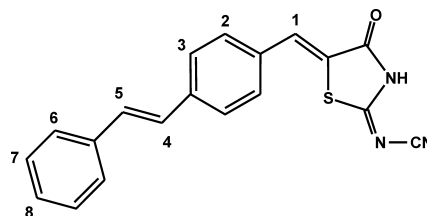


Fig. 1. Chemical Structure of 2-(*N*-Cyanoimino)-5- $\{$ (*E*)-4-styrylbenzylidene $\}$ -4-oxothiazolidine (FPFS-410) and Proton Numbering

\* To whom correspondence should be addressed. e-mail: uekama@gpo.kumamoto-u.ac.jp

complexation. Among them, 2-hydroxypropyl- $\beta$ -CyD (HP- $\beta$ -CyD) and sulfobutyl ether  $\beta$ -CyD (SBE7- $\beta$ -CyD) have been successfully applied to several poorly water-soluble drugs and their preparations are clinically used today. In this study, we compared the solubilization effect of CyDs on FPFS-410 and investigated the interaction of FPFS-410 with HP- $\beta$ -CyD which had the largest solubilizing effect on the compound. Further, the dissolution rate and *in-vivo* absorption behavior of FPFS-410/HP- $\beta$ -CyD complex in dogs were investigated in comparison with those of FPFS-410 alone.

## Experimental

**Materials**  $\alpha$ -CyD,  $\beta$ -CyD,  $\gamma$ -CyD, HP- $\alpha$ -CyD (degree of substitution (DS) 4.0), HP- $\beta$ -CyD (DS 4.8) and HP- $\gamma$ -CyD (DS 4.2) were obtained from Nihon Shokuhin Kako Co. (Tokyo, Japan), and SBE7- $\beta$ -CyD (DS 6.2) was donated by CyDex Inc. (KS, U.S.A.). FPFS-410 was designed and synthesized by Fujimoto Pharmaceutical Co. (Osaka, Japan). Deuterium oxide ( $D_2O$ , 99%) was purchased from Aldrich Chem. Co. (Milwaukee, WI, U.S.A.). Other chemicals and solvents were of analytical reagent grade and double-distilled water was used throughout the study.

**Solubility Studies** The solubility method was carried out according to the method of Higuchi and Connors.<sup>17)</sup> An excess amount of FPFS-410 (about 1 mg) was added in the screw-capped vials (1.5 ml) containing CyDs solutions at various concentrations in 1.0 M phosphate buffer (pH 7.0). The vials were shaken at 25 °C. After equilibrium was attained (about 3 d), the solution was centrifuged ( $5500\times g$ , 15 min), filtered through a cotton plug, and analyzed for FPFS-410 by high-performance liquid chromatography (HPLC). The HPLC conditions were as follows: a Hitachi L-6000 pump (Tokyo, Japan) and a Hitachi L-4000 UV detector at 390 nm (Tokyo, Japan); a Hitachi D-2500 ChromatoIntegrator (Tokyo, Japan); a GL-Sciences Nucleosil C18 ODS column ( $4.6\times 250$  mm, Tokyo, Japan); a mobile phase of acetonitrile/0.05 M ammonium acetate aqueous solution (11 : 9 v/v); a flow rate of 0.80 ml/min. It was confirmed that there is no change in pH of solutions before and after the equilibrium. The 1 : 1 stability constants ( $K_{1:1}$ ) of the complexes were calculated from an initial straight line portion of phase solubility diagrams with Eq. 1<sup>17)</sup>:

$$K_{1:1} = \frac{\text{slope}}{S_0(1 - \text{slope})} \quad (1)$$

where  $S_0$  and slope represent the intrinsic solubility of FPFS-410 and the slope of the phase-solubility diagram, respectively. On the other hand, the positively deviated diagrams were analyzed by the previously reported equations that are derived on the basis of the consecutive inclusion equilibrium, using a non-linear least-squares method (MULTI program) coupled with the iterative method, to obtain the  $K_{1:1}$  and  $K_{1:2}$  (guest : host) stability constants.<sup>18,19)</sup> The curve fitting was evaluated with a reference of Akaike's Information Criterion (AIC, the smaller AIC value means the better fit)<sup>20)</sup> and were  $-180$ — $-200$ . The solubility of FPFS-410 at acidic regions (pH < 5) was too low to measure accurately using HPLC ( $pK_a$  of FPFS-410: 3.4).

**<sup>1</sup>H-NMR Spectroscopic Studies and Molecular Modeling** <sup>1</sup>H-NMR spectra were taken at 25 °C on a JEOL JNM-ECP500 (Tokyo, Japan) operating at 500 MHz, using a 5-mm sample tube. 1.0 M deuterated phosphate buffer/ $D_2O$  (pH meter reading of 7.0) was used as a solvent and the water signal as an internal reference for <sup>1</sup>H-NMR. Chemical shifts were expressed in parts per million (ppm) relative to that of the HOD signal (4.65 ppm from sodium 2,2-dimethyl-2-silapentane-5-sulfonate), with an accuracy of  $\pm 0.001$  ppm. The assignment of <sup>1</sup>H-NMR signals of FPFS-410 was performed by correlation spectroscopy (COSY). The <sup>1</sup>H-NMR signals of HP- $\beta$ -CyD were assigned according to the reference.<sup>21)</sup> It was difficult to measure the NMR spectrum of FPFS-410 alone, because of its low solubility in water. Therefore, the spectra of FPFS-410 (1.5 mM) were taken after FPFS-410 was dissolved in HP- $\beta$ -CyD solutions (30, 60 mM). The phase-sensitive ROESY spectra were acquired with F1 and F2 spectral widths of 400—3800 Hz with 36 scans. The relaxation delay was 4.0 s, the 90° pulse width was 19.5  $\mu$ s, the spin-lock mixing time was set to 250 ms. The concentrations of FPFS-410 and HP- $\beta$ -CyD were 15 and 150 mM, respectively. Molecular docking simulations of the FPFS-410/ $\beta$ -CyD complex were carried out using a MOE-AS Dock software (Molecular Operating Environment, Chemical Computing Group Inc., Montreal, Canada; Ryoka System Inc., Tokyo, Japan). The geometry parameters of parent  $\beta$ -CyD were taken from the pre-

vious paper,<sup>22)</sup> and those of FPFS-410 were constructed with Chem3D software (Cambridge Soft, Cambridge, MA, U.S.A.). Various possible depositions (about 1000) and orientations of the guest molecule in the  $\beta$ -CyD cavity were generated using the program ASDock, and each structure was energy-minimized by the MMFF94x force field calculation to obtain the total energy ( $U_{\text{total}}$ ), the electrostatic and van der Waals interactions between the guest and  $\beta$ -CyD ( $U_{\text{ele}}$ ,  $U_{\text{vdw}}$ , respectively) and the conformation energy of the ligand ( $U_{\text{ligand}}$ ).<sup>23)</sup>

**Preparation of Solid Complex of FPFS-410 with HP- $\beta$ -CyD** Physical mixtures were prepared by simply mixing powder of each component using an agate mortar and a pestle in molar ratios of 1 : 1, 1 : 3 and 1 : 5 (FPFS-410 : HP- $\beta$ -CyD). Kneading products were prepared by triturating both components with ethanol and then kneading the slurry thoroughly for 1 h. The products were dried under reduced pressure at room temperature for about 3 d. Spray drying products were prepared by dissolving both components in ethanol/dichloromethane (1 : 1 v/v) and then spray-dried. The spray-drying was performed in a Pulvis GA-32 Yamato spray-drier (Tokyo, Japan) with an air flow rate of 0.4 m<sup>3</sup>/min, an air pressure of 1.0 kgf/cm<sup>2</sup>, inlet and outlet temperatures of 85 °C and 55 °C, respectively. Cogrounding products were prepared by grinding both components in a Fritsch pulverisette 6 (Idar-Oberstein, Germany) for 10 min at 100 $\times g$ .

**Powder X-Ray Diffraction Studies** Powder X-ray diffraction patterns were obtained with a Rikagaku CN 4037A1 X-ray diffractometer (Tokyo, Japan) with a Ni filtered CuK $\alpha$  radiation, a voltage of 30 kV, a current of 10 mA, a scanning speed of 1°/min, a time constant of 2 s, and a scan range of  $2\theta = 5$ — $30^\circ$ .

**Dissolution Studies** The dissolution rate of FPFS-410/HP- $\beta$ -CyD complexes was measured according to the paddle method in the Japanese Pharmacopoeia JP XIV. The powder sample (<200 mesh, equivalent to 5 mg FPFS-410) was added to the JP XIV second fluid (pH 6.8, 50.0 mM KH<sub>2</sub>PO<sub>4</sub> and 23.6 mM NaOH, 500 ml) and stirred at 100 rpm at 37 °C. At appropriate intervals, an aliquot of the dissolution medium was withdrawn using a pipette with a cotton plug. The volume in the vessel was replaced with the fresh dissolution medium after each sampling. The HPLC analysis was performed under the same conditions described above.

**Pharmacokinetic Studies in Dogs** Male beagle dogs weighing (9—11 kg) were fasted for 24 h prior to administration, while water was allowed *ad libitum*. The solid complex or FPFS-410 alone (equivalent to 20 mg/body) was filled in gelatin capsule and orally administered with water (50 ml) using a catheter. In the case of intravenous injections, FPFS-410 was completely dissolved in 1.0 M phosphate buffer (pH 7.0) containing HP- $\beta$ -CyD (150 mM), and was given at a dose of 20 mg/kg. Blood samples (about 1 ml) were taken periodically from the proleg vein using a heparinized injection syringe and centrifuged at  $5500\times g$  for 3 min at 4 °C. FPFS-410 was extracted from the plasma (0.3 ml) by ethyl acetate (5.0 ml) containing an internal standard (*p*-nitrophenol,  $3.6\times 10^{-5}$  M). The organic phase (4.0 ml) was evaporated under reduced pressure and the residue was redissolved in 0.1 ml of the mobile phase, 0.05 ml of which was subjected to HPLC analysis. The HPLC analysis was performed under the same conditions described above. The bioavailability parameters were calculated by the model-independent moment analysis according to the method of Yamaoka *et al.*<sup>24)</sup>

**Statistical Analysis** Data are given as means  $\pm$  standard error of the mean (S.E.M.). Statistical significance of mean coefficients was determined by analysis of variance followed by Student's *t*-test with  $p < 0.05$  considered to be statistically significant.

## Results and Discussion

**Solubility Studies** Figure 2 shows the phase solubility diagrams of FPFS-410 with parent  $\alpha$ -,  $\beta$ - and  $\gamma$ -CyDs, HP- $\alpha$ -, HP- $\beta$ - and HP- $\gamma$ -CyDs, and SBE7- $\beta$ -CyD in 1.0 M phosphate buffer (pH 7.0) at 25 °C. The phase solubility diagram of parent  $\alpha$ -CyD with FPFS-410 showed an A<sub>L</sub> type diagram under the experimental conditions, *i.e.*, the solubility of the guest increased linearly with increasing CyD concentrations.  $\beta$ -CyD gave an A<sub>p</sub> type diagram, where the solubility deviated positively from a straight line at higher CyD concentrations, indicating a formation of 1 : 1 and higher order 1 : 2 complexes (guest : host).  $\gamma$ -CyD gave a B<sub>s</sub> type diagram, precipitating solid complex at higher CyD concentrations. HP- $\alpha$ -CyD, HP- $\beta$ -CyD and HP- $\gamma$ -CyD showed A<sub>p</sub> type dia-

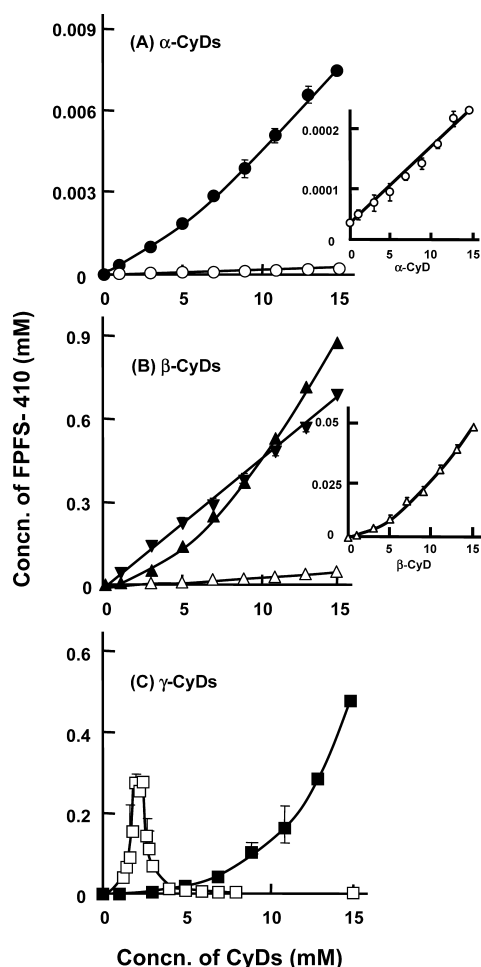


Fig. 2. Phase Solubility Diagrams of FPFS-410/ $\alpha$ -CyDs (A), FPFS-410/ $\beta$ -CyDs (B) and FPFS-410/ $\gamma$ -CyDs (C) Systems in 1.0 M Phosphate Buffer (pH 7.0) at 25 °C

(○)  $\alpha$ -CyD (or inserted figure), (●) HP- $\alpha$ -CyD, (△)  $\beta$ -CyD (or inserted figure), (▲) HP- $\beta$ -CyD, (▼) SBE7- $\beta$ -CyD, (□)  $\gamma$ -CyD, (■) HP- $\gamma$ -CyD. Each point represents the mean  $\pm$  S.E. of 3 experiments. The solid lines were the theoretical curves for the 1:1 and 1:2 complexations, except for the parent  $\gamma$ -CyD system.

grams, with significant increase in solubility of FPFS-410 at higher CyD concentrations, whereas SBE7- $\beta$ -CyD gave an  $A_L$  type diagram. Table 1 summarizes the stability constants ( $K_{1:1}$ ,  $K_{1:2}$ ) obtained by the analysis of the solubility curves (see Experimental). It is apparent that  $\alpha$ -CyD,  $\beta$ -CyD and their hydroxypropylated derivatives form predominantly the 1:1 complexes with FPFS-410 under these CyD concentration ranges, because the  $K_{1:1}$  values are much larger than the  $K_{1:2}$  values, and parent  $\alpha$ -CyD and SBE7- $\beta$ -CyD showed  $A_L$  type solubility diagrams. The  $K_{1:1}$  values of the parent  $\beta$ -CyD and HP- $\beta$ -CyD complexes ( $3.36 \times 10^4 \text{ M}^{-1}$ ,  $6.02 \times 10^5 \text{ M}^{-1}$ , respectively) were larger than those of the corresponding  $\alpha$ -CyDs complexes ( $4.38 \times 10^2 \text{ M}^{-1}$ ,  $1.14 \times 10^4 \text{ M}^{-1}$ , respectively), suggesting a higher affinity of  $\beta$ -CyD than  $\alpha$ -CyD to FPFS-410. Further, the  $K_{1:1}$  values of the hydroxypropylated  $\alpha$ - and  $\beta$ -CyD complexes were higher than those of the corresponding parent CyD complexes, suggesting a higher affinity of the hydroxypropylated CyDs than the parent CyDs to FPFS-410. When compared between the HP- $\beta$ -CyD and SBE7- $\beta$ -CyD complexes, the  $K_{1:1}$  value ( $1.48 \times 10^6 \text{ M}^{-1}$ ) of the SBE7- $\beta$ -CyD complex was higher than that ( $6.02 \times 10^5 \text{ M}^{-1}$ ) of the HP- $\beta$ -CyD. However, when

Table 1. Stability Constants ( $K_{1:1}$  and  $K_{1:2}$ )<sup>a)</sup> of FPFS-410/CyD Complexes in 1.0 M Phosphate Buffer (pH 7.0) at 25 °C

System	$K_{1:1} (\text{M}^{-1})$	$K_{1:2} (\text{M}^{-1})$
$\alpha$ -CyD	$4.38 \times 10^2$	—
$\beta$ -CyD	$3.36 \times 10^4$	$1.41 \times 10^2$
$\gamma$ -CyD	$3.22 \times 10^2$	$4.20 \times 10^6$
SBE7- $\beta$ -CyD (D.S., 6.2) <sup>b)</sup>	$1.48 \times 10^6$	—
HP- $\alpha$ -CyD (D.S., 4.0) <sup>b)</sup>	$1.14 \times 10^4$	40
HP- $\beta$ -CyD (D.S., 4.8) <sup>b)</sup>	$6.02 \times 10^5$	$1.46 \times 10^2$
HP- $\gamma$ -CyD (D.S., 4.2) <sup>b)</sup>	19	$3.40 \times 10^6$

a)  $K_{1:1}$  and  $K_{1:2}$ : stability constants of 1:1 and 1:2 (guest: host) complexes, respectively. S.E. <10% of the mean. b) The average degree of substitution.

1:1 and 1:2 complexations are both considered, the apparent affinity ( $K_{1:1} \times K_{1:2} = 8.79 \times 10^7 \text{ M}^{-2}$ ) of HP- $\beta$ -CyD was higher than that of SBE7- $\beta$ -CyD ( $1.48 \times 10^6 \text{ M}^{-1}$ ), which was reflected in their solubilizing abilities, *i.e.*, the solubility-enhancing effect of SBE7- $\beta$ -CyD on FPFS-410 was higher than that of HP- $\beta$ -CyD at lower CyD concentrations (Fig. 2B), whereas it was reversed at higher CyD concentrations. In the case of the  $\gamma$ -CyD complexes, the  $K_{1:2}$  values were significantly larger than the  $K_{1:1}$  values, indicating that FPFS-410 forms predominantly the 1:2 (guest: host) complexes with parent  $\gamma$ -CyD and HP- $\gamma$ -CyD under the experimental conditions. Both  $K_{1:1}$  ( $3.22 \times 10^2 \text{ M}^{-1}$ ) and  $K_{1:2}$  ( $4.20 \times 10^6 \text{ M}^{-1}$ ) values of the parent  $\gamma$ -CyD complex were larger than those of the HP- $\gamma$ -CyD complex. However, parent  $\gamma$ -CyD showed the  $B_S$  type solubility diagram with FPFS-410, precipitating the solid complex at higher CyD concentrations, and the FPFS-410/ $\gamma$ -CyD complex had limited solubility in water, *i.e.*, the maximum solubility of the compound in the presence of  $\gamma$ -CyD was about 0.3 mM. The order of solubilizing ability of CyDs toward FPFS-410 at a concentration of 15 mM CyDs was  $\gamma$ -CyD  $\ll$   $\alpha$ -CyD  $<$   $\beta$ -CyD  $<$  HP- $\alpha$ -CyD  $\ll$  HP- $\gamma$ -CyD  $<$  SBE7- $\beta$ -CyD  $<$  HP- $\beta$ -CyD. Among CyDs employed, HP- $\beta$ -CyD had the highest solubilizing ability to FPFS-410, *e.g.*, the low solubility of FPFS-410 ( $2.8 \times 10^{-8} \text{ M}$  in 1.0 M phosphate buffer (pH 7.0) at 25 °C) increased about 200000-fold at 40 mM HP- $\beta$ -CyD (data not shown), which was attributable to the formation of the 1:2 (guest: host) inclusion complexes. Therefore, we selected HP- $\beta$ -CyD as a solubilizer for FPFS-410 and used it in the following studies.

#### <sup>1</sup>H-NMR Spectroscopic Studies of FPFS-410 with HP- $\beta$ -CyD

<sup>1</sup>H-NMR spectroscopic studies were conducted to gain insight into the inclusion mode of the FPFS-410/HP- $\beta$ -CyD complex in aqueous solution. By the addition of FPFS-410 (1.5 mM), the inner H3' proton of HP- $\beta$ -CyD (60 mM) significantly shifted upfield (0.058 ppm), whereas the outer H1', H2', H4' and methyl protons of the 2-hydroxypropyl group shifted negligibly (data not shown). Unfortunately, the inner H5' proton of HP- $\beta$ -CyD could not be quantitatively monitored because of the overlapping with other protons. These results suggest that the guest is included in the HP- $\beta$ -CyD cavity. On the other hand, by the addition of HP- $\beta$ -CyD, homogeneous chemical shift changes were observed in almost all protons of FPFS-410, *i.e.*, large shifts in the H2, H3, H4 and H5 protons (0.02, 0.012, 0.008, 0.008 ppm downfield displacements, respectively) and small shifts in the H1 and H6 protons (0.003 upfield and 0.002 ppm downfield displacements, respectively). These results suggest that FPFS-410 is



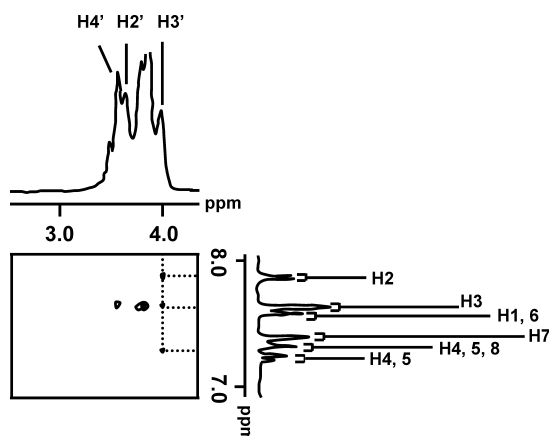


Fig. 3. Partial Contour Plot of ROESY Spectrum of FPFS-410/HP- $\beta$ -CyD System in Deuterated Phosphate Buffer (pH Meter Reading of 7.0) at 25 °C

The concentrations of FPFS-410 and HP- $\beta$ -CyD were 15 and 150 mM, respectively.

fully included in two HP- $\beta$ -CyD cavities in aqueous solution. The inclusion complexation of FPFS-410 with HP- $\beta$ -CyD complex was studied by ROESY spectroscopic method. As shown in Fig. 3, the correlation peaks were observed between the H2, H3, H4 and H5 protons of the guest and the inner H3' proton of the host in the spectrum obtained. These results suggest that the central benzene and oxothiazolidine moieties of the drug is located in the HP- $\beta$ -CyD cavity to form the 1 : 2 complex.

**Molecular Modelling** Because the aqueous solubility of FPFS-410 was too low to study in detail the complexation by means of spectroscopic methods, we estimated the inclusion mode of the 1 : 2 complex by molecular modelling. Figure 4 shows the MOE-optimized structure of the FPFS-410/ $\beta$ -CyD complexes in a molar ratio of 1 : 2. The docking calculation was conducted using parent  $\beta$ -CyD instead of HP- $\beta$ -CyD, because HP- $\beta$ -CyD is a multi-component mixture of structurally related compounds. The top- to forth-rank models estimated by the docking calculation gave the almost identical inclusion structure with similar  $U_{\text{total}}$ ,  $U_{\text{ele}}$ ,  $U_{\text{vdw}}$  and  $U_{\text{ligand}}$  energy levels, *i.e.*, (−8.44—−7.23), (−13.5—−10.1), (−26.9—−31.5) and (32.4—33.4) kcal/mol, respectively. As shown in Fig. 4, the H4 and H5 protons in addition to the H2 and H3 protons of the guest are located near the secondary hydroxyl side of  $\beta$ -CyD. This inclusion structure was coincided with the ROESY spectrum, providing the correlation peaks between the H2—H5 protons of the guest and the H3' proton of the host. It is reasonable to assume that the 1 : 2 FPFS-410/HP- $\beta$ -CyD complex has the similar structure to that of the  $\beta$ -CyD complex (Fig. 4), because both  $\beta$ -CyDs gave the  $A_p$  type of phase solubility diagram in 1.0 M phosphate buffer.

**Preparation of Solid Complex of FPFS-410 with HP- $\beta$ -CyD** The solid complexes of FPFS-410/HP- $\beta$ -CyD in different molar ratios (1 : 1, 1 : 3, 1 : 5) were prepared by the physical mixing, kneading, spray-drying and cogrinding methods (see Experimental). Figure 5 shows diffraction patterns of FPFS-410/HP- $\beta$ -CyD systems. FPFS-410 gave sharp diffraction peaks at  $2\theta=9.3$ , 13.2, 14.6 and 26.3°, indicating high crystallinity of the compound. The physical mixtures (patterns b—d in Fig. 5) and kneading products (patterns e—g in Fig. 5) of FPFS-410/HP- $\beta$ -CyD gave several peaks of

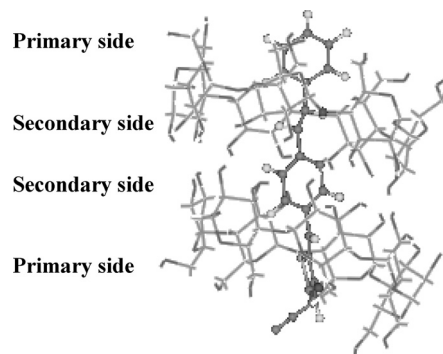


Fig. 4. Inclusion Structure of FPFS-410/ $\beta$ -CyD Complex in a 1 : 2 Stoichiometry Estimated by Docking Model Calculation

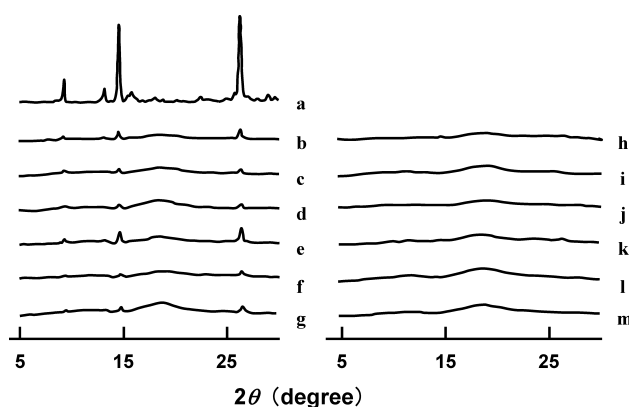


Fig. 5. Powder X-Ray Diffraction Patterns of FPFS-410/HP- $\beta$ -CyD Systems

(a) FPFS-410 alone; physical mixtures of FPFS-410 and HP- $\beta$ -CyD (b) 1 : 1, (c) 1 : 3, (d) 1 : 5; kneading products of FPFS-410 and HP- $\beta$ -CyD (e) 1 : 1, (f) 1 : 3, (g) 1 : 5; cogrinding products of FPFS-410 and HP- $\beta$ -CyD (h) 1 : 1, (i) 1 : 3, (j) 1 : 5; spray-drying products of FPFS-410 and HP- $\beta$ -CyD (k) 1 : 1, (l) 1 : 3 and (m) 1 : 5.

FPFS-410. During the kneading, concentrating and drying processes, FPFS-410/HP- $\beta$ -CyD complex may dissociate to each component, because of the high crystallinity of FPFS-410. On the other hand, the spray drying products and the cogrinding products gave a halo-pattern and the diffraction peaks of the guest disappeared (patterns h—m in Fig. 5), indicating that FPFS-410 forms an amorphous solid complex with HP- $\beta$ -CyD.

**Dissolution Studies** It is well known that dissolution of solid drugs is the rate-limiting step for gastrointestinal absorption of poorly water-soluble drugs. Therefore, the dissolution behavior of FPFS-410 in the JP XVI second fluid (pH 6.8) was investigated. The solubility ( $1.9 \times 10^{-7}$  M at 37 °C) of FPFS-410 in this dissolution medium was higher than that of the solubility diagram, because of the increased temperature and the different salt concentration. As shown in Fig. 6, amounts of the drug dissolved from the kneading products were lower when compared with those of the spray-drying and cogrinding products, and were comparable to those of the physical mixtures, because FPFS-410 is in crystalline state in the HP- $\beta$ -CyD matrix, as suggested from X-ray diffraction studies. On the other hand, the amorphous FPFS-410/HP- $\beta$ -CyD complexes prepared by the spray drying and cogrinding methods exhibited the fast dissolution, and it increased as the molar ratio of HP- $\beta$ -CyD increased. Amounts of the drug dissolved from the cogrinding products were

slightly lower than those of the spray drying products, which may be due to the massive aggregation of ground fine powders during the cogrinding process.<sup>25)</sup> Therefore, the FPFS-410/HP- $\beta$ -CyD complex was prepared by the spray-drying

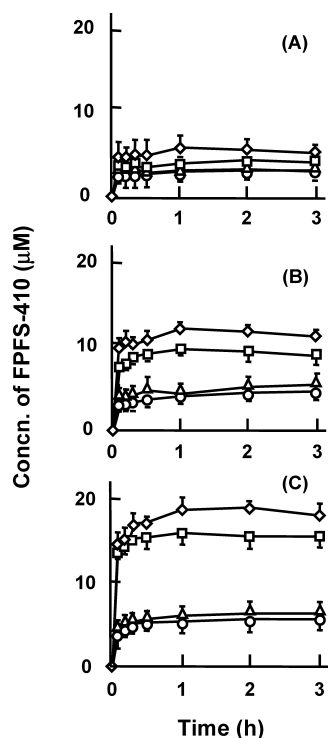


Fig. 6. Dissolution Profiles of FPFS-410/HP- $\beta$ -CyD Complexes in Different Molar Ratios of 1 : 1 (A), 1 : 3 (B) and 1 : 5 (C) in JP XIV Second Fluid (pH 6.8) at 37 °C

(○) physical mixtures, (△) kneading products, (□) cogrinding products, (◇) spray drying products. Each point represents the mean  $\pm$  S.E. of 3 experiments.

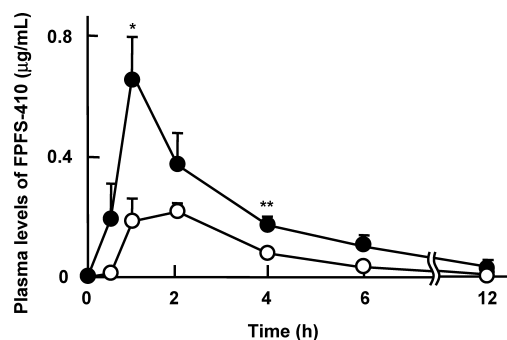


Fig. 7. Plasma Levels of FPFS-410 after Oral Administration of FPFS-410 Alone and Its HP- $\beta$ -CyD Complex (Equivalent to 20 mg/Body FPFS-410) to Dogs

(○) FPFS-410 alone, (●) 1 : 5 complex. Each point represents the mean  $\pm$  S.E. of 3 experiments. \*  $p < 0.05$  versus alone, \*\*  $p < 0.01$  versus alone.

method and used in the following *in-vivo* absorption studies.

**Pharmacokinetic Studies in Dogs** The enhanced solubility and dissolution of FPFS-410 by the HP- $\beta$ -CyD complexation were reflected in the *in-vivo* absorption behavior in dogs. Figure 7 shows plasma levels of FPFS-410 after oral administration of solid FPFS-410 alone or FPFS-410/HP- $\beta$ -CyD complex (in a molar ratio of 1 : 5) filled in a gelatin capsule. The pharmacokinetic parameters are listed in Table 2. In comparison with FPFS-410 alone, the HP- $\beta$ -CyD complex gave higher plasma levels of FPFS-410, *e.g.*, the levels at 1 h were  $0.675 \pm 0.123$   $\mu\text{g/ml}$  (the complex) and  $0.186 \pm 0.076$   $\mu\text{g/ml}$  (FPFS-410 alone) and those at 4 h were  $0.173 \pm 0.011$   $\mu\text{g/ml}$  (the complex) and  $0.079 \pm 0.005$   $\mu\text{g/ml}$  (FPFS-410 alone). Further, the  $AUC_{0-12}$  and  $F$  values of the complex were about 3 times greater than those of FPFS-410 alone. The enhancement of bioavailability of FPFS-410 by the complexation with HP- $\beta$ -CyD was rather smaller than that expected from the results of the dissolution rates (Fig. 6), which may be due to differences between *in-vitro* and *in-vivo* experimental conditions such as amounts of gastrointestinal tract and agitation speeds, as well as due to the metabolism of FPFS-410 in the gastrointestinal membrane and liver.

## Conclusions

The newly synthesized FPFS-410 has both antidiabetic and lipid-lowering activities without unwelcome effects. However, the aqueous solubility of FPFS-410 is extremely low, preventing development of various dosage forms. In this study, we attempted to improve the solubility and oral bioavailability of FPFS-410 by means of the complexation with CyD, and investigated the interaction of FPFS-410 with HP- $\beta$ -CyD in aqueous solution. HP- $\beta$ -CyD markedly enhanced the solubility of FPFS-410 at higher CyD concentrations, *e.g.*, the 200000-fold increase of the solubility by the addition of 40 mM HP- $\beta$ -CyD. The enhanced solubility was attributable to the formation of the 1 : 2 (guest : host) inclusion complexes. Further, the increased solubility and dissolution were reflected in the *in-vivo* absorption in dogs. The present results suggest that HP- $\beta$ -CyD is useful in designing oral solid preparations of FPFS-410 for improving gastrointestinal absorption.

## References

- 1) Reaven G. M., *Diabetes*, **37**, 1595—1607 (1988).
- 2) Lillioja S., Mott D. M., Spraul M., Ferraro R., Foley J. E., Ravussin E., Knowler W. C., Bennett P. H., Bogardus C., *N. Eng. J. Med.*, **329**, 1988—1992 (1993).
- 3) Miyazaki Y., Mahankali A., Matsuda M., Mahankali S., Hardies J., Cusi K., Mandarino L. J., Defronzo R. A., *J. Clin. Endocrinol. Metab.*, **87**, 2784—2791 (2002).
- 4) Iozzo P., Hallsten K., Oikonen V., Virtanen K. A., Parkkola R., Kempainen J., Solin O., Lonnqvist F., Ferrannini E., Knuuti J., Nuutila P.,

Table 2. Pharmacokinetic Parameters of FPFS-410 after Oral Administration of FPFS-410 Alone and Its Complex (Equivalent to 20 mg/Body) to Dogs

System	$AUC_{0-12h}$ ( $\mu\text{g} \cdot \text{h/ml}$ )	$C_{max}$ ( $\mu\text{g/ml}$ )	$T_{max}$ (h)	MRT (h)	$F^a$ (%)
FPFS-410 alone	$0.74 \pm 0.05$	$0.25 \pm 0.02$	$1.67 \pm 0.33$	$3.30 \pm 0.19$	$5.14 \pm 0.35$
FPFS-410/HP- $\beta$ -CyD (molar ratio 1/5)	$2.05 \pm 0.16^*$	$0.68 \pm 0.12$	$1.00 \pm 0.00$	$3.45 \pm 0.67$	$14.18 \pm 1.08^*$

a) The extent of bioavailability compared with the  $AUC$  value of intravenously administered FPFS-410. The  $F$  values were determined using data upto 12 h postadministration. Each value represents the mean  $\pm$  S.E. of 3 experiments. \*  $p < 0.05$  versus alone.

- Diabetes Care*, **26**, 2069—2074 (2003).
- 5) Aronoff S., Rosenblatt S., Braithwaite S., Egan J. W., Mathisen A. L., Schneider R. L., *Diabetes Care*, **23**, 1605—1611 (2000).
  - 6) Lebovitz H. E., Dole J. F., Patwardhan R., Rappaport E. B., Freed M. I., *J. Clin. Endocrinol. Metab.*, **86**, 280—288 (2001).
  - 7) Saltiel A. R., Olefsky J. M., *Diabetes*, **45**, 1661—1669 (1996).
  - 8) Grossman S. L., Lessem J., *Expert Opin. Investig. Drugs*, **6**, 1025—1040 (1997).
  - 9) Ciraldi T. P., Huber-Knudsen K., Hickman M., Olefsky J., *Metabolism*, **44**, 976—982 (1995).
  - 10) Spiegelman B. M., *Diabetes*, **47**, 507—514 (1998).
  - 11) Scheen A. J., *Diabetes Metab.*, **27**, 305—313 (2001).
  - 12) Wang C. H., Weisel R. D., Liu P. P., Fedak P. W. M., Verma S., *Circulation*, **107**, 1350—1354 (2003).
  - 13) Norisada N., Masuzaki H., Fujimoto M., Inoue G., Hosoda K., Hayashi T., Watanabe M., Muraoka S., Yoneda F., Nakao K., *Metabolism*, **53**, 1532—1537 (2004).
  - 14) Stella V. J., Rajewski R. A., *Pharm. Res.*, **14**, 556—567 (1997).
  - 15) Hirayama F., Uekama K., *Adv. Drug Deliv. Rev.*, **36**, 125—141 (1999).
  - 16) Uekama K., *Chem. Pharm. Bull.*, **52**, 900—915 (2004).
  - 17) Higuchi T., Connors K. A., *Adv. Anal. Chem. Instr.*, **4**, 117—212 (1965).
  - 18) Higuchi T., Kristiansen H., *J. Pharm. Sci.*, **59**, 1601—1608 (1970).
  - 19) Yamaoka K., Tanigawara Y., Nakagawa T., Uno T., *J. Pharmacobio-Dyn.*, **4**, 879—885 (1981).
  - 20) Akaike H., *Psychometrika*, **52**, 317—332 (1987).
  - 21) Miyake K., Irie T., Arima H., Hirayama F., Uekama K., Hirano M., Okamoto Y., *Int. J. Pharm.*, **179**, 237—245 (1999).
  - 22) Ikeda Y., Motoune S., Matsuoka T., Arima H., Hirayama F., Uekama K., *J. Pharm. Sci.*, **91**, 2390—2398 (2002).
  - 23) Goto J., Kataoka R., Hirayama N., *J. Med. Chem.*, **47**, 6804—6811 (2004).
  - 24) Yamaoka K., Nakagawa T., Uno T., *J. Pharmacokinet. Biopharm.*, **6**, 547—558 (1978).
  - 25) Shakhshneider T. P., Boldyrev V. V., *Molecular Solid State*, **3**, 271—311 (1999).